01 Jan 1976

# Bit Penetration Into Rock-A Finite Element Study

J. K. Wang

T. F. Lehnhoff
*Missouri University of Science and Technology*, lehnhoff@mst.edu



## Recommended Citation

J. K. Wang and T. F. Lehnhoff, "Bit Penetration Into Rock-A Finite Element Study," *International Journal of Rock Mechanics and Mining Sciences and*, vol. 13, no. 1, pp. 11 - 16, Elsevier, Jan 1976.
The definitive version is available at https://doi.org/10.1016/0148-9062(76)90222-9

Int. J. Rock Mech. Min. Sci. & Geomech. Abstr. Vol. 13, pp. 11–16. Pergamon Press 1976. Printed in Great Britain

# Bit Penetration into Rock—A Finite Element Study

J. K. WANG*
T. F. LEHNHOFF†

*The sequence of rock failure mechanisms and quantitative information on stress, displacement and material failure in the process of bit penetration have been obtained through computer simulation. A finite element approach has been developed to simulate bit penetration from bit rock interaction to chip formation. A mathematical rock failure model, based on available rock failure experiments, has been proposed to represent post-failure rock behavior and applied in the penetration simulations. The finite element code was developed for two-dimensional plane strain problems to consider non-linear material properties, geometric non-linearity, and fracture propagation. An anistropic element as well as variable stiffness and stress release methods have been used. An iteration method, using an incremental displacement approach, has been applied for continuous penetration with modification of material properties and displacements. The simulation results of the blunt point bit are in reasonable agreement with penetration experiments on Limestone. Wedge and cylinder bit profiles have also been presented to demonstrate their shape effects.*

## INTRODUCTION

Basic studies on bit penetration into rock have been of interest to many investigators in recent years [1,2]. Much of the past success has been achieved through experimentation, and some empirical models for brittle chip formation rock have been introduced. They generally cover some important events in the failure sequence, however, they rarely describe the details of chip formation and give no quantitative evaluation of the stress and displacement field during the penetration process. The simplified models also neglect the effects of some important post-failure material properties.

The primary difficulty of an analytical study of bit penetration lies in the fact that the constitutive theories, which are generally applied for describing rock behavior in the elastic state, become inadequate for the fractured rock. The complexity of the post-failure character of rock makes our task for a general constitutive law and its solution practically impossible at present.

The purpose of this study is primarily to develop a general mathematical rock failure model and along with the available finite element techniques to establish a computer code, which will allow the simulation of the sequence of penetration mechanisms and provide a better description of the failure phases—initial cracking, crushing, and chipping. The code can also be used for the study of the effects of tool shapes and material properties.

* Design Engineer, Brown & Root, Inc., Houston, TX, U.S.A.
† Assoc. Prof., University of Missouri—Rolla, MO, U.S.A.

## MATHEMATICAL MATERIAL FAILURE MODEL FOR ROCK

In the interest of studying practical engineering problems, a mathematical model based on observations of experimental results is proposed [2].

1. Before the stress state reaches the maximum failure strength, rock is considered linear-elastic, isotropic and homogeneous.

2. As shown in the results of many experimental tests, the maximum strength of an intact rock can be approximated by a linear Mohr envelope as shown in Fig. 1. Rock failure occurs when the Mohr circle of a stress state of rock reaches the envelope. The shape of the linear envelope can be determined by its tensile and compressive strengths and the slope of the envelope. The transition between tensile and compressive failures can be determined by the following relations:

$$\sigma = \frac{1}{2\tau_0\mu}\tau^2 + \sigma_t, \qquad \tau_0 = \frac{\sigma_c \cos\theta}{2(1+\sin\theta)} \tag{1}$$

where $\mu$, $\sigma_t$, $\sigma_c$ and $\tau_0$ are the slope of the Mohr envelope, tensile strength, compressive strength, and intrinsic shear strength respectively.

3. After tensile fracture, rock loses its cohesion on the newly created surface and still retains its strength in the direction parallel to the fracture surface.

4. After compressive failure, rock strength and stiffness decrease gradually along with displacements until they finally approach a minimum value corresponding to the residual strength [3–6]. Degrees of failure are represented by dividing the space between two extreme

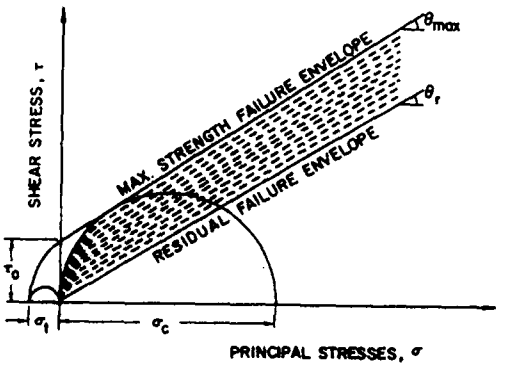


Fig. 1. Idealized failure envelope for rock.

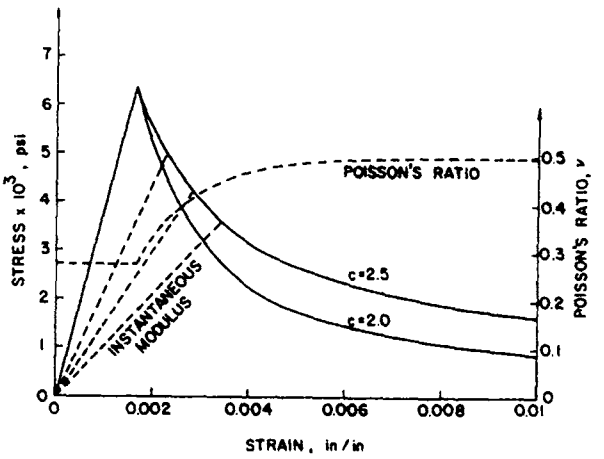


Fig. 2. Idealized stress–strain curves for salem Limestone.

envelopes, intact and residual, into many levels. On each level, i.e. the same failure envelope, the degree of failure and material properties are assumed the same.

Because the study of the post-failure behavior of rock is still in the developing stage, knowledge of material properties after failure is very limited. Some interpolations between bounded values and extrapolations from the available properties are necessary.

Since the stiffness of rock decreases with displacement, the instantaneous value of Young's modulus for a fractured rock is assumed to be the slope of the chord of the stress–strain curve as shown in Fig. 2. A simple mathematical relation, representing this characteristic, can be expressed as

$$E_i = E\left(\frac{\sigma_i - \sigma_r}{\sigma_{max} - \sigma_r}\right)^c \tag{2}$$

where $E_i$ = instantaneous stiffness, $c$ = slope constant, $\sigma_i$ = instantaneous strength, $\sigma_{max}$ = maximum strength, $\sigma_r$ = residual strength.

Figure 2 shows two post-failure stress–strain curves with constants $c = 2$ and 2·5. These two values are used in the penetration simulations.

As the stiffness of rock decreases in progressive failure, Poisson's ratio should also be changed accordingly. Since Poisson's ratio for fractured rock is not available, an alternative approach is suggested. If the compressibility of a rock is constant before and after failure, then Poisson's ratio becomes a function of the instantaneous stiffness $E_i$. The variable Poisson's ratio is given as:

$$\nu_i = \frac{1}{2}\left[1 - \frac{E_i}{E}(1 - 2\nu)\right]. \tag{3}$$

Figure 2 illustrates the change of Poisson's ratio along the stress–strain curve. Material properties of Indiana Limestone are listed in Table 1 [8].

## THE FINITE ELEMENT METHOD AND ITS APPLICATION FOR PENETRATION SIMULATION

In order to associate the finite element method with the proposed mathematical failure model as described in the previous section, some finite element techniques will be used in the simulation [7,9]. An anisotropic element is introduced to represent an element after tensile failure. Variable stiffness is used in the simulation of progressive strength failure of rock. A stress release technique and iteration method are applied during the process of continuous penetration.

Bit penetration studies of long wedge (or blunt point) bit acting on a large block of rock can be considered a plane strain problem without considering the end effects.

### 1. *Anisotropic element*

When the minor principal stress of an element reaches its critical value in tension, a fracture surface is created perpendicular to the principal direction. This newly developed surface imposes an additional boundary to the system and results in a significant stress redistribution in the immediate vicinity as well as a change in the structure stiffness. The simulation procedure can be accomplished by assuming that the crack plane is a principal plane for the anisotropic element. In the direction normal to the plane, Young's modulus and Poisson's ratio are reduced to very small values. Nevertheless, the element is still capable of withstanding stress parallel to the crack plane. The plane strain elasticity matrix, $[D]$, for a symmetric anisotropic ele-

TABLE 1. MATERIAL PROPERTIES OF INDIANA LIMESTONE USED IN THIS STUDY

| | |
|---|---|
| Tensile strength, $\sigma_t$ | -759 psi |
| Compressive strength, $\sigma_c$ | 6,370 psi |
| Young's modulus, E | 3,660,000 psi |
| Poisson' ratio, ν | 0.272 |
| Angle of maximum Mohr envelope, $\theta_{max}$ | 30 degrees |
| Residual angle of Mohr envelope, $\theta_r$ | 25 degrees (1st model)* |
| | 30 degrees (2nd model) |
| Slope constant, c | 2.0 (1st model) |
| | 2.5 (2nd model) |

*The 1st model is used in all bits, the 2nd model is used with a blunt point bit only.

ment can be expressed as:

$$[D] = \frac{E_2}{(1+\nu_1)(1-\nu_1-2n\nu_2^2)} \times \begin{bmatrix} n(1-n\nu_2^2) & n\nu_2(1+\nu_1) & 0 \\ n\nu_2(1+\nu_1) & (1-\nu_1^2) & 0 \\ 0 & 0 & m(1+\nu_1) \\ & & (1-\nu_1-2n\nu_2^2) \end{bmatrix} \quad (4)$$

where $n = \frac{E_1}{E_2}$, and $m = \frac{1}{2(1+\nu_2)}$.

The constant $E_1$ and $\nu_1$ are associated with the behavior in the fracture plane, and $E_2$ and $\nu_2$ with a direction normal to these.

2. *Non-linear material properties*

For non-linear material problems, the stiffness matrix of each element is a function of its stress or strain level. Therefore, the final stiffness matrix $[K]$ of the whole structure can be expressed as

$$[K(\{\sigma\})]\{\delta\} = \{R\} \quad \text{or} \quad [K(\{\epsilon\})]\{\delta\} = \{R\}. \quad (5)$$

The above equations can be solved by iterative methods. In order to study successive penetration, the incremental displacement method is used. Rewriting the above equation in terms of small penetration increments, we obtain

$$[K]_{n-1}\{\Delta\delta\}_n = \{\Delta R\}_n \quad (6)$$

where $[K]_{n-1}$ is the stiffness matrix at the previous stress state, and $\{\Delta\delta\}_n$ and $\{\Delta R\}_n$ are matrices of small incremental displacement and nodal loads.

3. *Geometric non-linearity*

Equation (6) has been derived based on small displacements with non-linear material properties. For problems with large displacements or strains, assuming the geometry of elements remains unchanged and using first-order, infinitesimal linear strain approximations may yield an inaccurate solution. Using the iteration method as suggested in equation (6), adjustment for this geometric non-linearity can be accomplished by redefining element coordinates in the computation of stiffnesses. Rewriting equation (6) we have

$$[K(\delta,\sigma)]_{n-1}\{\Delta\delta\}_n = \{\Delta R\}_n \quad (7)$$

where $[K(\delta,\sigma)]_{n-1}$ is the stiffness matrix formulated by the most recent coordinates of the elements.

It should be noted that not all non-linearities are accounted for in this study. But since bit penetration is conducted on a large block of rock and large strains, which occur at the edges of a bit, are not possible without fracture, significant errors are not introduced [7].

4. *Stress release*

Zienkiewicz *et al.* have suggested a so called 'stress transfer' method to study linear elastic rock behavior by considering rock as a 'no tension' material [9]. The method converts excessive stresses that an element cannot bear to nodal loads and re-applies these nodal loads to the system, i.e. excessive stresses can be released from an over stressed element to neighboring elements. Assuming $\{\Delta\delta\}^e$ are the excessive stresses in an element, then the transformation for nodal loads $\{\Delta R\}^e$ is given by:

$$\{\Delta R\}^e = \int_e [B]^T\{\Delta\sigma\}^e\, dV. \quad (8)$$

5. *Iteration process*

Simulation of bit penetration starts from the initial contact of a bit and an intact rock without pre-existing stresses. A small assigned incremental penetration is imposed in each iteration to obtain incremental stresses. If the displacement increment is sufficiently small, then each incremental solution may be considered linear and could be accomplished accurately in one step. In order to trace actual fracture propagation, the computer program is designed to adjust the penetration magnitude in each iteration by allowing no more than one unfailed element to reach the failure envelope. The ratio of the adjusted penetration to the assigned penetration is used in calculating actual incremental stresses. After the accumulated total stresses for each element are obtained, the stress states of all failed elements are checked to determine their current situation. Further modifications for material properties and releases for excessive stresses follow, if necessary. An additional loop within the same iteration is performed to release these excessive stresses. In this loop, transformation from stresses to nodal loads is accomplished using equation (8), and the incremental penetration is taken as zero. Stress redistribution is accomplished at the end of this loop by adding the incremental stresses, generated from the transferred nodal loads, to the total stresses of all elements.

Since the incremental displacement is small, modification for geometric non-linearity is taken after a specified number of iterations, $n$. A simplified flow chart of the program is shown in Fig. 3. Detailed information on the program is presented in reference [9].

6. *Simulations*

Blunt point, sharp wedge and cylindrical bits are used in the penetration simulations. A rough bit-rock interface is assumed for all cases, i.e. no relative movement on the contact surface between bit and rock. The overall size and the imposed boundary conditions of the grid are comparable with the experimental test conducted by Maurer [1].

*Blunt point bit*—A series of plots showing principal stresses, degrees and types of element failure and position of elements at various stages of penetration of blunt point bit, using the first material model, are illustrated from Figs. 4a–4c. Rock begins to fail after a small elastic deformation at the boundary of the cutting edge, where high stress intensity exists. Major principal stresses in all elements are in compression with directions toward the penetrating bit. Elements immediately

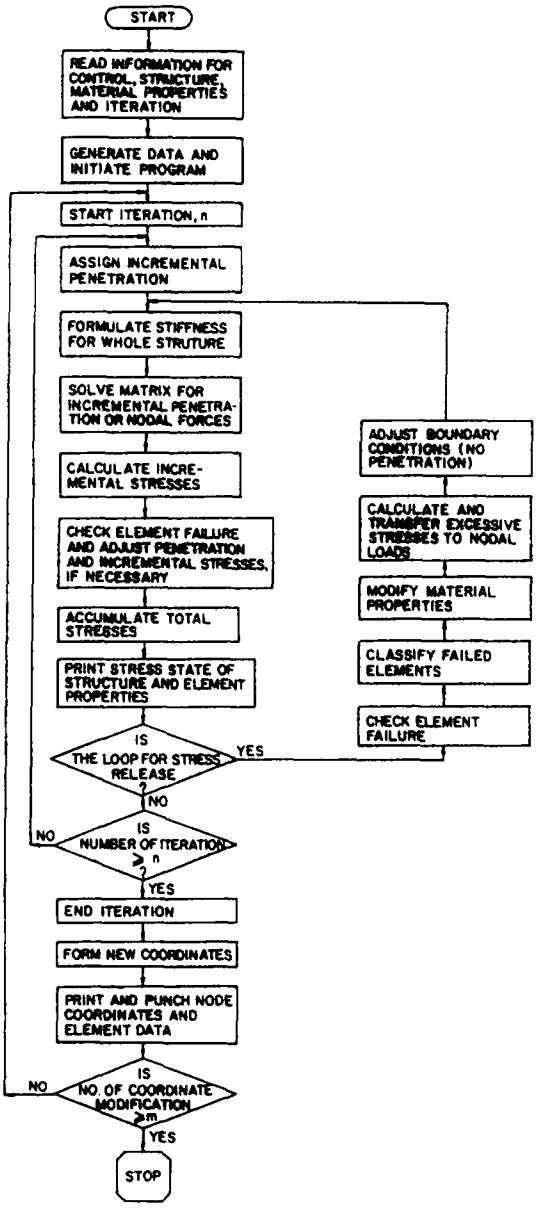


Fig. 3. Flow chart for bit penetration simulation.

under the bit have high compressive minor principal stresses which keep these elements in the elastic state. The highest stress intensity elements at this stage are under the cutting edge. Fracture in the rock propagates from the edge downward a certain distance creating a central high compressive zone and separating it from two sides of the rock as shown in Fig. 4a. As the penetration continues, the failed area expands toward the symmetric center of the rock and forms a compressive failure zone surrounding a small portion of the high compressive elastic area immediately under the bit. Increasing penetration at this point has little effect on the side elements, but gradually reduces material strength and stiffness of the compressive zone. The elements which have failed in compression, under the pressure of the penetrating bit, are squeezed into lateral movement and as a consequence tensile fractures start from the bottom of the compressive zone and gradually spread to both sides as shown in Fig. 4b. If the penetration is further increased, the increasing pressure on the side elements will reach the point that fractures start to propagate in these elements and finally form a chip, as shown in Fig. 4c. The corresponding force–displacement curve of this penetration simulation is plotted in Fig. 5. Cross marks on the curve indicate the positions of bit penetration, where stress field and element failure are plotted. Every dot represents an iteration in the computer program. As shown in Fig. 5, the force–penetration curve of this simulation is lower than the experimental result, however, the depths of bit penetration at the peaks of both curves, where the first chip is formed, are close. The analytical F–P curve at the beginning of the penetration showing a steeper

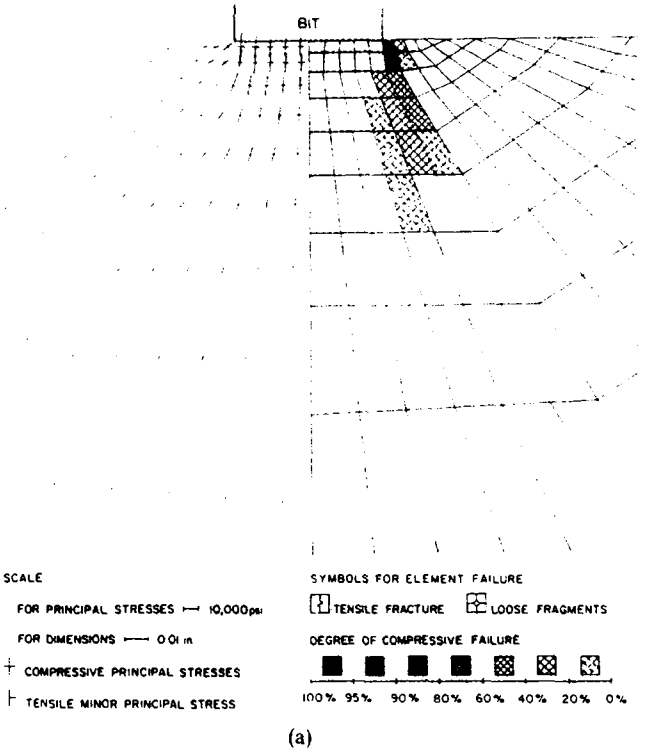


(a)

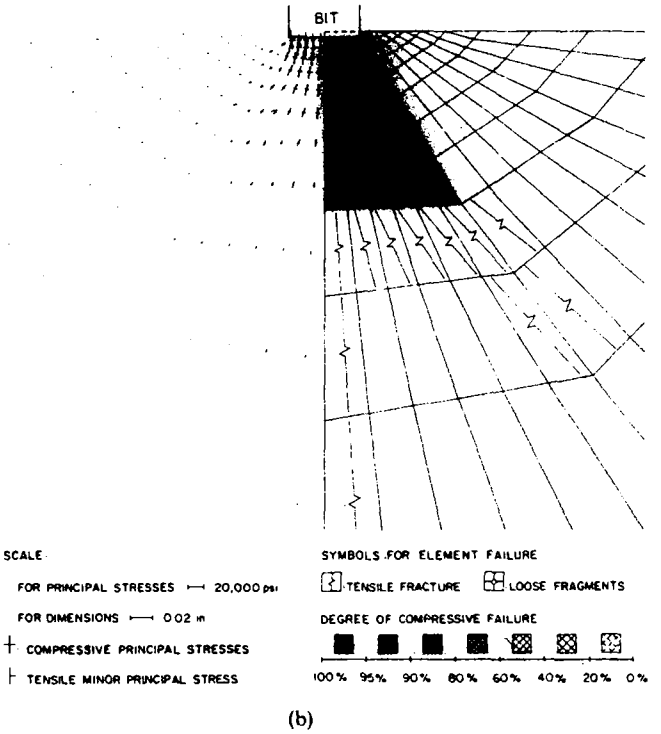


(b)

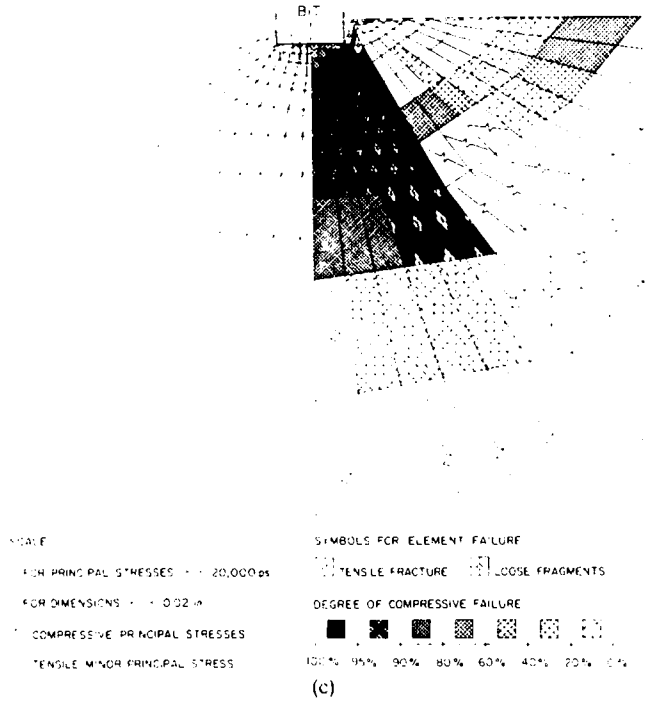


(c)

Figs. 4 (a–c). Blunt point bit penetration using the first material model.

slope is probably due to the linear-elastic assumption for rock before failure.

Figure 5 also shows the blunt point bit penetration, using the second material failure model of higher post-failure strength. Some differences between the two simulations are observed: (a) the depth of penetration to form the chip is greater in the second simulation, (b) the degrees of failure of the elements in the compressive zone are more homogeneous, and (c) the F–P curve in Fig. 5 for the second simulation is higher than the curves of the first simulation and the experimental result. These results demonstrate the influence of the post-failure rock behavior and properties on bit penetration.

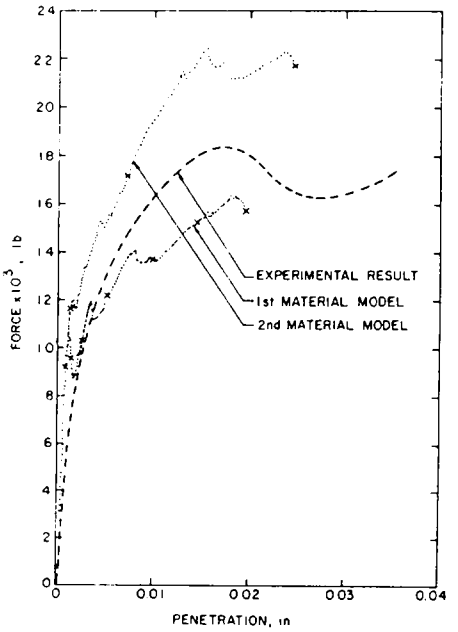


Fig. 5. Force-penetration curves for blunt point bit.

*Sharp wedge bit.* The initial position of the bit starts with a dent in the rock. Only one element makes contact with the bit at the beginning of this simulation. Additional contact area will be added, if the bit starts to reach other elements.

As shown in Fig. 6a, the compressive failure zone quickly spreads from the edge of the wedge to the area under the bit. The tensile crack under the compressive failure zone starts to propagate before the side elements have developed high enough pressure to form a chip. The final stage of this simulation is shown in Fig. 6b and the F–P curve is given in Fig. 7.

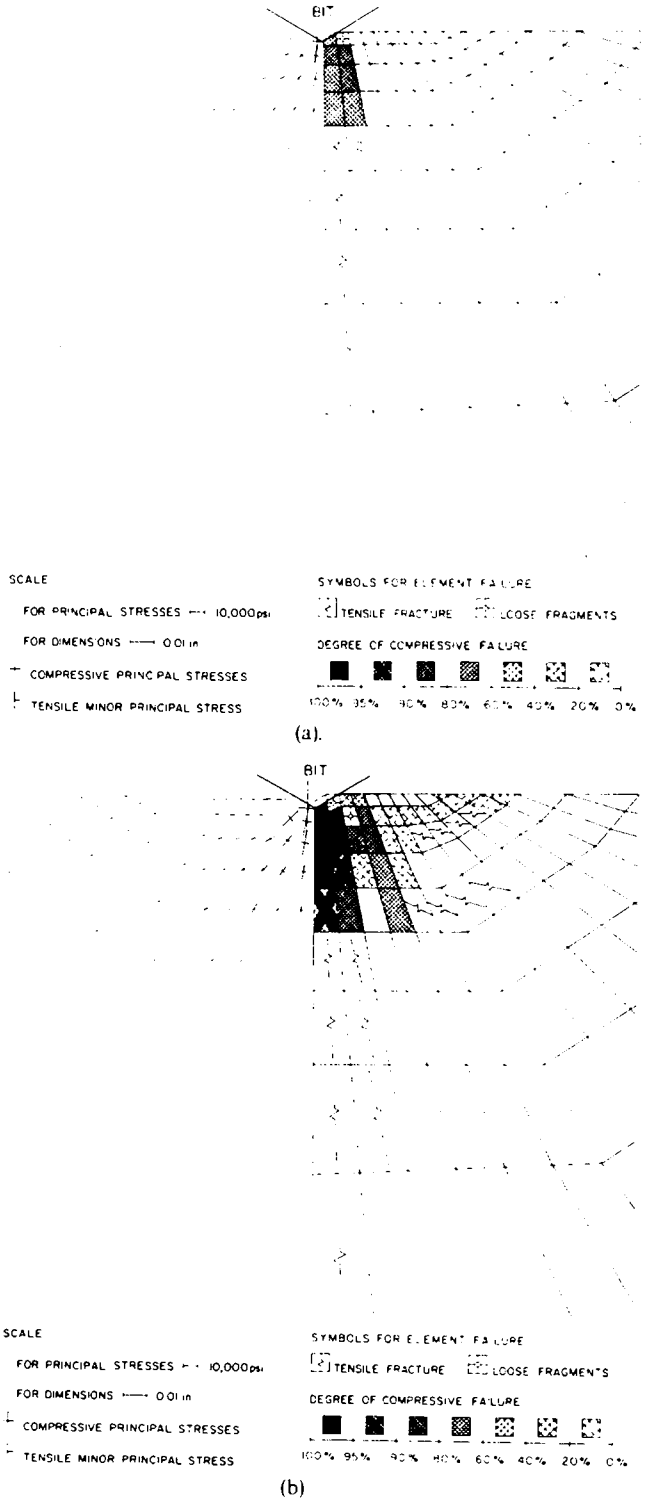


(a).

(b)

Figs. 6 (a and b). Sharp wedge bit penetration.

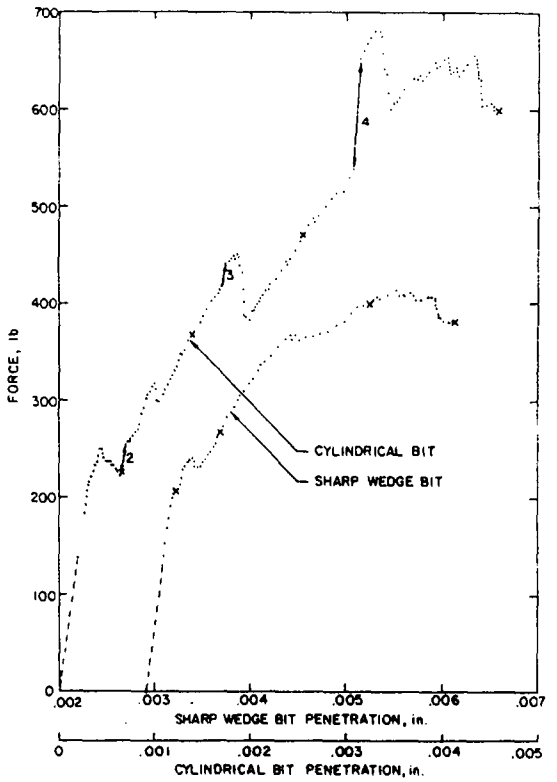


Fig. 7. Force-penetration curves for sharp wedge and cylindrical bits.

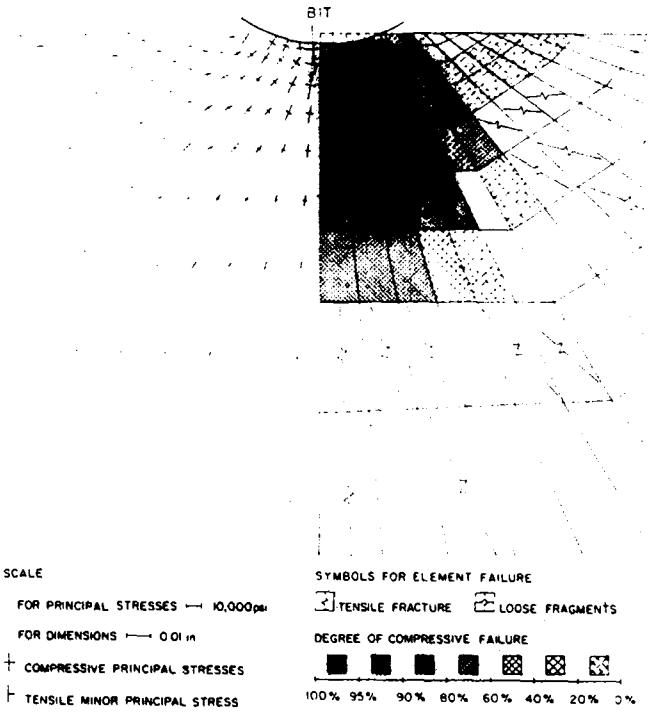


Fig. 8. Cylindrical bit penetration.

A wedge bit, with the action of the inclined bit surfaces, creates quicker lateral pressure on the side elements, which results in early chip formation and more effective bit penetration.

*Cylindrical bit.* The simulation starts from only one element making contact with the bit. Along with the continuing penetration and increasing contact surface with the bit, the compressive failure zone of the rock keeps expanding in the lateral and vertical directions. Final chip formation is shown in Fig. 8.

The F–P curve of this simulation shows a jump in applied force for every new element to contact the bit, as illustrated in Fig. 7. The number at each jump indicates the order of the new contact element. After the element at the edge of the contact zone decreases its strength with penetration, the increased force starts to fall as shown in the figure.

## CONCLUSIONS

Using the proposed mathematical rock failure model and the developed finite element code, the sequence of rock failure mechanisms and the quantitative information on stress, displacement and material failure in the process of bit penetration can be obtained. The analytical results presented in this study have shown reasonable agreement with experimental observations. Effects of tool shape (e.g. bit wear) and post-failure rock strength can be studied using the method.

**Acknowledgement**—This work was supported partially by grants NSF-GI-38984 and ARPA USDI H0220068.

*Received* 30 *May* 1975.

## REFERENCES

1. Maurer W. C. The state of rock mechanics knowledge in drilling. *Proc. 8th Symp. Rock Mech.*, Univ. of Minn., 355–395.
2. Sikarskie D. L. & Cheatham J. B., Jr. Penetration problems in rock mechanics. *Rock Mechanics Symposium, A.S.M.E., A.M.D.*, Vol. 3, pp. 41–71 (1974).
3. Bieniawski Z. T. Propagation of rittle fracture in rock. *Proc. 10th Sym. Rock Mech.*, Univ. of Texas—Austin (1968).
4. Hoek E. & Bieniawski Z. T. Brittle fracture propagation in rock under compression, *Int. J. Fract. Mech.* **1**, 137–155 (1965).
5. Barnard P. R. Reasearches into the complete stress–strain curve for concrete *Mag. Concr. Res.* **16**, 203–210 (1964).
6. Deere D. V. *et al.* Design of surface and near-surface construction in rock. *Proc. 8th Sym. Rock Mech.*, Minn (1966).
7. Zienkiewicz O. C. The finite element method. McGraw-Hill, London (1971).
8. Krech W. W. *et al.* A standard rock suite for rapid excavation research. BuMines RI 7865 (1974).
9. Wang J. K. Bit penetration into rock—A finite element study. Ph.D. Thesis, Univ. of MO—Rolla (1975).